AD-A094 390 MATERIALS RESEARCH LABS ASCOT VALE (AUSTRALIA) F/G 11/6
HIGH-TEMPERATURE OXIDATION OF NIMONIC 105 AT SUB-ATMOSPHERIC OX--ETC(U)
OCT 80 G R JOHNSTON
UNCLASSIFIED MRL-R-789 NL

1 OF 1
AD A
094390

END
DATE
FILMED
2-81
DTIC

MRL-R-789 (12) AR-002-369

AD A094390

DEPARTMENT OF DEFENCE

DEFENCE SCIENCE AND TECHNOLOGY ORGANISATION

MATERIALS RESEARCH LABORATORIES

MELBOURNE, VICTORIA

REPORT

MRL-R-789

HIGH-TEMPERATURE OXIDATION OF NIMONIC 105 AT SUB-ATMOSPHERIC OXYGEN PARTIAL PRESSURES

Graham R. Johnston

Approved for Public Release

A

FILE COPY

[illegible]
[illegible]
[illegible]
[illegible] AND [illegible]

DEPARTMENT OF DEFENCE
MATERIALS RESEARCH LABORATORIES

REPORT

14 **MRL-R-789**

6 HIGH-TEMPERATURE OXIDATION OF NIMONIC 105 AT SUB-ATMOSPHERIC OXYGEN PARTIAL PRESSURES

Graham R. Johnston

11 Oct 81

ABSTRACT

12 34

This report describes studies of some high-temperature oxidation characteristics of the wrought superalloy Nimonic 105. This work is related to the development of a high-temperature brazing process for military gas-turbine aerofoil components involving gaseous atmospheres of very low oxygen activity.

Approved for Public Release

A

POSTAL ADDRESS: Chief Superintendent, Materials Research Laboratories
P.O. Box 50, Ascot Vale, Victoria 3032, Australia

409014

DOCUMENT CONTROL DATA SHEET

Security classification of this page: UNCLASSIFIED

1. *DOCUMENT NUMBERS:*
   a. *AR Number:* AR-002-369
   b. *Series & Number:* REPORT MRL-R-789
   c. *Report Number:* MRL-R-789

2. *SECURITY CLASSIFICATION:*
   a. *Complete document:* UNCLASSIFIED
   b. *Title in isolation:* UNCLASSIFIED
   c. *Abstract in isolation:* UNCLASSIFIED

3. *TITLE:*

HIGH-TEMPERATURE OXIDATION OF NIMONIC 105 AT
SUB-ATMOSPHERIC OXYGEN PARTIAL PRESSURES

4. *PERSONAL AUTHOR(S):*

JOHNSTON, Graham R.

5. *DOCUMENT DATE:* OCTOBER, 1980

6. *TYPE OF REPORT & PERIOD COVERED:*

7. *CORPORATE AUTHOR(S):*

Materials Research Laboratories

8. *REFERENCE NUMBERS:*
   a. *Task:* DST 77/064
   b. *Sponsoring Agency:*

9. *COST CODE:* 554860

10. *IMPRINT (Publishing establishment)*

Materials Research Laboratories,
P.O. Box 50, Ascot Vale, Vic. 3032
OCTOBER, 1980

11. *COMPUTER PROGRAMME(S):*
(Title(s) and language(s)):

12. *RELEASE LIMITATIONS (of the document):*

Approved for Public Release

12-0. *OVERSEAS:* N.O. ☐ P.R. 1 A ☐ B ☐ C ☐ D ☐ E ☐

13. *ANNOUNCEMENT LIMITATIONS (of the information on this page):*

No limitation

14. *DESCRIPTORS:*

630	Nickel alloys	Brazing	Oxidation	
645	High temperature	Gas turbine engines	Nimonic 105	

15. *COSATI CODES:* 0702 1106 1308

16. *ABSTRACT (if this is security classified, the announcement of this report will be similarly classified):*

This report describes studies of some high-temperature oxidation characteristics of the wrought superalloy Nimonic 105. This work is related to the development of a high-temperature brazing process for military gas-turbine aerofoil components involving gaseous atmospheres of very low oxygen activity.

CONTENTS

HIGH TEMPERATURE OXIDATION OF NIMONIC 105 AT SUB-ATMOSPHERIC OXYGEN PARTIAL PRESSURES

1. INTRODUCTION

This report describes an investigation of the high-temperature oxidation characteristics of the wrought nickel-base superalloy Nimonic 105 in atmospheres of low partial pressures of oxygen. The work was undertaken to assist in solving problems encountered in the development in Australia of high-temperature brazing techniques for fabricating components for military gas-turbine engines.

2. BACKGROUND

In gas-turbine aeroengine technology the technique of high-temperature brazing is widely used to join complex alloys that are virtually unweldable or to fabricate complicated assemblies that are impractical to weld.

All the Nimonic alloys can be furnace brazed, either in vacuum or in a controlled-atmosphere which produces a very low oxygen partial pressure. The stable and tenacious oxide films formed on aluminium- and titanium-containing Nimonic alloys are not readily reduced in vacuum and, if an adequate flow of the brazing alloy is to be achieved without the use of fluxes, pressures lower than 10 μm Hg ($\approx$1.4 Pa) would seem necessary for alloys such as Nimonic 105 [1].

Hydrogen atmospheres with very low partial pressures of oxygen offer the advantage for brazing that oxides already present on the surfaces to be joined might be reduced by such atmospheres at normal brazing temperatures.

3. THE PROBLEM

The present investigation relates to a problem, encountered with Rolls-Royce Avon 207 military turbojet engines, in producing brazed joints (brazements) between Nimonic 105 high-pressure turbine blades and their Nimonic 75 sealing plates.[1] The sealing plates are secured to the leading faces of the turbine blade fir-tree roots (Fig. 1) to protect them from direct impingement of the hot gas stream from the combustor.

The brazing process was carried out at the Commonwealth Aircraft Corporation (CAC), Melbourne, initially in an Ipsen vacuum furnace operating at nominal minimal pressures of approximately 0.5 μm Hg ($\approx 7 \times 10^{-2}$ Pa); this was in general accord with the relevant CAC procedural specification [3]. It was to be expected, therefore, that the brazements in question would be satisfactorily effected in this furnace. A significant number of these brazements in each furnace load, however, were found to be faulty and it was necessary either to reject them or to re-braze them. Inspection of rejected assemblies showed that a faulty brazement occurred where the oxide tarnish produced on a Nimonic 105 blade surface was visibly darker than that produced on the surface of a successfully joined component [4].

Failure to achieve both flow of brazing metal and adequate wetting of surfaces to be joined can be related to the degree of oxidation of these Nimonic surfaces which occurs during the heating cycle of the brazing operation [1]. Little information appears to be available in the literature on the high-temperature oxidation of the Nimonic alloys at these low oxygen pressures. High Temperature Properties Group MRL undertook, therefore, to investigate the high-temperature oxidation characteristics of the two Nimonic alloys, initially Nimonic 105, at various sub-atmospheric partial pressures of oxygen. The aim of this work was to determine whether surface oxidation was responsible for the brazing failures and, if so, to determine an alternative brazing procedure which would virtually suppress such oxidation and eliminate the problem.

4. EXPERIMENTAL

Some high-temperature oxidation characteristics of Nimonic 105 at various oxygen pressures were studied at MRL using a laboratory vacuum furnace which was programmed to reproduce the CAC brazing heat-treatment cycle, shown in Table 2. Samples were heated both in air at sub-atmospheric pressures and in a N_2-10% H_2 [2] atmosphere. Thermogravimetry and electron

---

[1] The chemical compositions of Nimonic 105 and Nimonic 75 are given in Table 1. Unless otherwise stated, all alloy compositions given in this paper are expressed as percentages by weight.

[2] Commercial-grade 'furnace' gas which contains 10 per cent hydrogen, by volume, in nitrogen.

probe microanalysis were used to characterize the oxides formed on these specimens. For comparison, similar characterizations were performed on samples which were heated in the CAC Ipsen furnace which was either fully evacuated or filled with a N_2-10% H_2 atmosphere. Auger electron spectroscopy was also used to identify oxides formed in air.

4.1 Sample Preparation

Test-samples of Nimonic 105 were prepared from new (unused) Rolls-Royce Avon turbine blades supplied by CAC. The aerofoil part of each blade was cut into several approximately equal sections, which were numbered consecutively and given a letter designation to distinguish the different blades. The samples were polished to P1200 grade paper, ultrasonically cleaned and vapour degreased. Prior to oxidation the weight and surface area of each sample were measured.

4.2 Oxidation Procedures

For the experiments in air, the MRL furnace was fully evacuated ($\simeq 7 \times 10^{-4}$ Pa) and the desired constant pressure of air was then established using a controlled-leak valve. Total pressure regulation of the order of ±25 per cent was attained over the complete heating cycle. One sample (D-17) was heated in air in the CAC furnace operating at its minimum pressure.

For the experiments in the N_2-10% H_2 atmosphere, two samples were heated in the MRL furnace at a total pressure of 1.3 Pa, and one was heated at about the same pressure in the CAC brazing furnace.

4.3 Analytical Procedures

4.3.1 Thermogravimetry

After exposure the oxidized samples were re-weighed to measure their gain in weight, from which the specific weight gain was calculated. From these results, estimates of the average oxide thickness (see Appendix) were made.

4.3.2 Electron probe microanalysis (EPMA)

The surfaces of the oxidized samples were analysed by EPMA. The EPMA technique employed utilized minimal electron-accelerating voltages ($\geqslant 3$ kV) to reduce the penetration depth of the incident electron beam and thus confine the depth of analysis to a minimum. An accelerating voltage of 3 kV was used for most of the analyses in this work.

4.3.3 Auger electron spectroscopy (AES)

The oxide layer on Sample C-10 was analysed by AES*. This was done because the EPMA results for the samples oxidized at the lower oxygen pressures were not conclusive. Even with the 3 kV accelerating voltage used in the EPMA, electron beam penetration of the thin oxide layers occurred which gave results showing anomalously high bulk-metal contributions. The greater depth resolution (≃0.5 nm) of the AES technique ensured that an analysis of the surface oxide film was obtained which was free from bulk-metal interference. The AES results were obtained using a 'depth profile' method whereby analyses were performed at a number of discrete depths below the original surface. In this method the surface is progressively eroded by a technique of ion milling.

5. RESULTS

5.1 Thermogravimetry

5.1.1 Oxidation in Air

The weight gains obtained by the oxidation of the Nimonic 105 samples at various pressures in air, using the CAC brazing heat-treatment temperature cycle (Table 2), are summarized in Table 3. The specific weight gain (w) was found to increase with increasing oxygen pressure (P_{O_2}) in the furnace. Figure 2 shows the dependence of w on P_{O_2}. A log-log scale was chosen for Figure 2 on the assumption that the dependence could be of the form:

$$w \propto P_{O_2}{}^{1/n} \text{ (i.e. } \log w \propto 1/n \log P_{O_2})$$

in accord with Wagner oxidation theory [5].

At a pressure of approximately 10^{-2} Pa, there is an apparent change in the dependence of w on P_{O_2}. Below 10^{-2} Pa, w changes more rapidly with P_{O_2} ($n \simeq 1.5$) than it does at oxygen pressures above 10^{-2} Pa ($n \simeq 10$).

---

* The AES analysis was performed by Messrs P.J.K. Paterson and V.B. Hill in the Physics Department, Royal Melbourne Institute of Technology.

5.1.2 *Oxidation in N_2-10% H_2 atmosphere*

Because the N_2-10% H_2 gas mixture was used directly from a commercial cylinder without attempting to remove its water vapour content, the oxygen pressure of the gas mixture was sufficient (Section 6.2) to oxidize the more reactive solute elements in Nimonic 105. The weights gained by the samples, when heated in this atmosphere at a total pressure of approximately 1.3 Pa, are given in Table 4. Again, the CAC brazing heat-treatment temperature cycle was used.

5.2 *Surface Characterization*

5.2.1 *Electron probe microanalysis (EPMA)*

EPMA was used to determine the composition of the oxides present on the samples heated in the two different atmospheres at discrete oxygen activities. The accelerating potential of the incident electron beam was reduced from its normal value of 20 kV to improve the depth resolution of the technique. This improvement is illustrated in Figure 3, where the measured element concentration is plotted as a function of accelerating potential. Whereas the 20 kV potential showed aluminium to be present at an apparent level of approximately 10%, the 3 kV potential clearly shows aluminium to be the major constituent of the surface oxide with all other metallic elements present at negligible levels.

Table 5 presents the EPMA results for the Nimonic 105 samples included in Table 3, namely those heated at various pressures in air. The measured concentrations of the six major elements - Ni, Co, Al, Ti, Cr and Mo - are presented for those samples on which EPMA analyses were performed. A beam voltage of 3 kV was used in all cases, with additional analyses at 7, 15 and 20 kV performed on some of the samples (e.g. Sample A-4). Table 5 also gives the apparent oxide compositions and the calculated oxide thickness (see Section 6.1.2 and Appendix).

Table 6 presents the EPMA results for the samples included in Table 4, namely those heated in the N_2-10% H_2 atmosphere.

5.2.2 *Auger electron spectroscopy (AES)*

An AES analysis was performed on Sample C-10 in an attempt to confirm that Al_2O_3 is formed, exclusively, on the surface of Nimonic 105 when heated in atmospheres of low oxygen partial pressure.

The atomic concentration C_x of an element X in the sample is given [6] by

$$C_x = I_x / I_{Ag} S_x \qquad (1)$$

where I_x is the peak-to-peak amplitude from the element X in the sample;

I_{Ag} is the peak-to-peak amplitude from a pure silver standard; and

S_x is the relative Auger sensitivity for element X.

Relative atomic percentage concentrations are obtained from

$$\frac{C_x}{\Sigma_{x=1}^{x=n} C_x} = \frac{I_x/S_x}{\Sigma_{x=1}^{x=n} (I_x/S_x)} \times 100$$

where the summations are over all the 'n' elements detected in the Auger spectrum.

Auger electron spectra are presented in Figures 4 and 5. The spectrum in Figure 4 was recorded after a short period of ion milling (48 s), while the spectrum in Figure 5 was recorded after 804 s of milling. Similar Auger spectra were also recorded at various intermediate times. Relative concentrations of the six major elements detected - Al, O, Ni, Co, Cr and C - are presented in Figure 6 as a function of ion milling time (i.e. milling depth). The concentration of carbon is anomalously high, particularly at the longer times. The high carbon levels detected probably result from re-deposition of carbon from heated surfaces adjacent to the area under analysis; if so, the carbon signals can be disregarded in the calculation of relative atomic concentrations. The concentration profiles thus calculated for the remaining five elements are shown in Figure 7. Figures 6 and 7 both indicate that the oxide film on the surface is exclusively an aluminium containing oxide, obviously Al_2O_3.

6. DISCUSSION

This work was undertaken to gain insight into the nature and mechanisms of the gas-metal reactions that occur when the superalloy Nimonic 105 is heated in atmospheres of various sub-atmospheric oxygen pressure during a high-temperature brazing cycle. The oxidation of Nimonic 105 in air at various oxygen pressures is discussed first, followed by a consideration of the heating of this alloy in an atmosphere of N_2-10% H_2. In conclusion, a resumê is given of the significance of these studies to the original brazing problem (see Section 3).

6.1 The Oxidation of Nimonic 105 in Air at Atmospheric Pressure and Sub-Atmospheric Pressures

6.1.1 Oxidation in air at atmospheric pressure

The oxidation mechanisms for the Nimonic series of alloys are discussed in general terms by Eggar [7]. The excellent oxidation resistance of these alloys is a consequence of the formation of protective surface oxides, such as Cr_2O_3 and Al_2O_3. Whether Al_2O_3 or Cr_2O_3 is the preferred scale in air depends on the relative amounts of the two elements in the alloy. For Nimonic 75, which is based on a Ni-20Cr binary alloy (refer Table 1), protection from continued oxidation is afforded mostly by layers of Cr_2O_3 and/or $NiCr_2O_4$ in the growing oxide scale. In the case of the more chemically-complex alloys of this type, such as Nimonic 105, Eggar [7] claims that the formation of Cr_2O_3 normally predominates in air, with Al_2O_3 being produced as an internal precipitate. The Al_2O_3 is then progressively incorporated in the thickening Cr_2O_3 scale.

Pettit et al. [8,9] report that a ternary Ni-15Cr-6Al alloy, heated in air at 1273 K for times in excess of 40 minutes develops a continuous, protective α-Al_2O_3 layer. At shorter exposure times, however, during transient stages of oxidation, 'islands' of both NiO and $Ni(Cr, Al)_2O_4$ spinels form as overlays on discontinuous areas of Cr_2O_3 and Al_2O_3. These oxide structures are formed because of the different diffusion rates of Ni, Cr and Al in both the base metal and the growing oxide scale [8,9].

In the present work, when Sample D-16 was subjected to the brazing temperature cycle in air at atmospheric pressure (i.e. $P_{O_2} \approx 2 \times 10^4$ Pa), a relatively thick oxide scale was formed consisting of at least two visually distinct regions. EPMA results (Table 5), identify two regions - one rich in Al, Ni, Co and Ti, and the other rich in Ni, Ti, Cr and Mo. The formation of oxide regions of different compositions on Nimonic 105 in air is consistent with the mechanism proposed by Pettit [8,9] for the transient oxidation of similar Ni-Cr-Al alloys.

6.1.2 Oxidation in air at sub-atmospheric pressures

For the oxidation of Nimonic 105 in various sub-atmospheric pressures of air, the degree of oxidation was found to decrease with decreasing oxygen pressure (Table 5 and Figure 2). Furthermore the chemical composition of the oxide scale changed when the pressure of oxygen was reduced below that of atmospheric pressure. At P_{O_2} values of 1.4 Pa and below, both EPMA and AES results indicate that the oxide films formed are composed almost exclusively of Al_2O_3, in contrast to the mixed oxides formed in air at atmospheric pressure (Section 6.1.1). Aluminium has a much greater affinity for oxygen (i.e. a larger negative free energy of oxide formation) than does any of the other major elements present in Nimonic 105. When the oxygen activity in the gas phase is reduced, aluminium oxidizes selectively to form Al_2O_3. It is presumably the thickness of this Al_2O_3 film that determines whether adequate flow of brazing metal, wetting of surfaces and joining will take place during the brazing of Nimonic 105 in vacuum-brazing operations.

The thickness of an oxide film formed on the surface of an alloy can be estimated from thermogravimetric determinations of its gain in weight during oxidation. A formula to convert specific weight gain (w) to oxide thickness (t) is derived in the attached Appendix. The calculated oxide thicknesses for samples in the present study are shown in Tables 5 and 6, using the value of 0.54 for the conversion factor for the single oxide Al_2O_3 (see Table 7).

The dependence of the degree of oxidation on P_{O_2} is shown in Figure 2. Two oxidation mechanisms appear to be indicated by the results, in that the specific weight gain (w) decreases more rapidly with decreasing P_{O_2}, at P_{O_2} values below approximately 10^{-3} Pa.

6.2 The Oxidation of Nimonic 105 in N_2-10% H_2 Atmosphere

Hydrogen is a reducing gas. In practice, however, traces of other gases (e.g. H_2O) are always present in commercially available hydrogen. If the amount of water vapour present in H_2 is carefully controlled, atmospheres with specific low partial pressures of oxygen can be generated through the equilibrium

$$H_2 + \tfrac{1}{2}O_2 \rightleftharpoons H_2O.$$

In the present tests, however, no attempts were made either to remove or to control the amount of water vapour present in the commercial N_2-10% H_2 atmospheres utilized.

Three Nimonic 105 test pieces were heated in N_2-10% H_2 atmospheres - Sample D-18 at CAC and Samples D-15 and D-19 at MRL (see Table 4). The magnitude of the specific weight gains that were measured for these samples indicates that the oxygen pressure in the N_2-10% H_2 atmosphere was in the region of 10^{-3} Pa (cf. Tables 3 and 4). The EPMA analyses for these samples (Table 6) are similar to those obtained for samples oxidized in air at sub-atmospheric pressures, and also consistent with an assumption of the presence of thin films of Al_2O_3 on the surface.

6.3 Significance to the Brazing Problem

The present study was undertaken to assist in solving problems associated with the brazing of Nimonic 75 sealing plates to Nimonic 105 turbine blades. The study attempted to determine the oxidation characteristics of Nimonic 105 in atmospheres having as wide a range of oxygen pressures as practicable, using the heat-treatment cycle stipulated for the brazing process under study.

From the study of the oxidation of Nimonic 105 at various pressures of oxygen, the following conclusions are drawn:

(i) the degree of oxidation decreased with decreasing oxygen pressure;

(ii) the rate of decrease of oxide formation was faster at P_{O_2} values below about 10^{-3} Pa; and

(iii) an exclusive Al_2O_3 film was formed in atmospheres with P_{O_2} values at or below about 1.4 Pa.

Vacuum-furnace brazing operations should therefore be performed at as low an oxygen pressure as practicable to minimize oxide formation which might produce faulty brazements. The one test sample (i.e. Sample D-17, Table 5), heated in the CAC vacuum-brazing furnace, had a specific weight gain on oxidation which corresponds to a low P_{O_2} value in the MRL series of tests, i.e. $P_{O_2} \approx 7 \times 10^{-4}$ Pa. This is at least three orders of magnitude lower than the pressure claimed to be necessary for the successful brazing of Nimonic alloys [1]. There is thus an apparent anomaly in that some brazements made at such a low pressure were unsuccessful. The explanantion may lie in the assumptions either that the previously published pressure requirement was too high or that the actual oxygen pressure in the CAC brazing furnace during routine operations was much higher than that obtaining in the furnace during the oxidation of the test specimen.

At the conclusion of this investigation MRL recommended to CAC that a N_2-10% H_2 atmosphere be used throughout the brazing cycle in their present vacuum-brazing furnace, in an attempt to improve the number of successful brazements. This recommendation was adopted by CAC, and subsequent brazements exhibited satisfactory joint quality in all respects [10], with rejection rates maintained below an average of five per cent [11].

7. ACKNOWLEDGEMENTS

The author is grateful to Messrs P.J.K. Paterson and V.B. Hill, Applied Physics Department, RMIT, for carrying out the Auger Electron Spectroscopy analysis; and to Mr R.M. Hess, High Temperature Properties Group, MRL, for general experimental assistance.

8. REFERENCES

1. Payne, B.E. (1974). 'Joining' in '*The Nimonic Alloys and Other Nickel-Base High-Temperature Alloys*' (eds. W. Betteridge and J. Heslop) pp.413-418, Edward Arnold (Publishers) Limited, London.

2. Morley, M. (1974). 'The Range of Alloys'. *ibid.*, p.24.

3. CAC Master Technique Card, No. 806A, 'Heat Treat Operations', June 1977.

4. Collins, M.R. Chief Materials and Process Engineer, Commonwealth Aircraft Corporation Ltd, Melbourne. Private Communication.

5. Kofstad, P. (1966). '*High Temperature Oxidation of Metals*', pp.124-129, J. Wiley and Sons, New York.

6. Paterson, P.J.K. and Wright, P.W. (1979). 'Some Metallurgical Applications of Auger Electron Spectroscopy'. *Metals Forum,* 2, 55-65.

7. Eggar, J.W. (1974). 'Corrosion Properties' in '*The Nimonic Alloys and Other Nickel-Base High-Temperature Alloys*' (eds. W. Betteridge and J. Heslop) pp. 342-352, Edward Arnold (Publishers) Limited, London.

8. Giggins, C.S. and Pettit, F.S. (1971). 'Oxidation of Ni-Cr-Al Alloys Between 1000° and 1200°C'. *J. Electrochem. Soc.*, 18, 1782-1790.

9. Kear, B.H., Pettit, F.S., Fornwalt, D.E. and Lemaire, L.P. (1971). 'On the Transient Oxidation of a Ni-15Cr-6Al Alloy', *Oxid. Metals,* 3, 557-569.

10. Theckston, A. (1977). 'Evaluation of Nimonic 105 Avon Turbine Blade Assemblies BR 78025 Following Brazing in a 10% Hydrogen, 90% Nitrogen Atmosphere at Ten Microns Total Pressure'. Commonwealth Aircraft Corporation Ltd., Melbourne, Laboratory. Report No. 1191.

11. Marion, J.L. (1977). 'Hydrogen Brazing of Rolls Royce Turbine Blades'. Commonwealth Aircraft Corporation Ltd., Melbourne, Interim Report LT 1985.

APPENDIX

CALCULATION OF OXIDE THICKNESS FROM THERMOGRAVIMETRIC RESULTS

When an oxide scale is formed on the surface of a metal sample during oxidation, the weight of the sample increases if oxygen uptake exceeds volatilization loss. When volatilization loss is negligible, therefore, the gain in weight can be regarded as a direct measure of the amount of oxygen in the oxide scale. It is therefore possible to calculate the oxide thickness (t) if the chemical identity and density (ρ) of the oxide is known. In this section, an attempt is made to generate a general formula to calculate t if the chemical nature of the oxide is unknown.

For a metal or alloy that forms a single oxide, M_xO, if w is the specific weight gain (i.e. the weight of O/unit area) the total specific weight of the oxide formed is

$$w\left(1 + \frac{x\,M'}{16}\right),$$

where M' is the atomic weight of the metal anion. If this oxide scale is assumed to be uniformly thick over the entire surface of the metal, then the thickness (t) of oxide is given by

$$t = \frac{w}{\rho}\left(1 + \frac{x\,M'}{16}\right)$$

where ρ is the density of the oxide M_xO. It is therefore possible to calculate t from w, if ρ and x are known. For an alloy that forms a mixed oxide $(M_1)_x(M_2)_yO$, where M_1 and M_2 are two metallic elements of atomic weight M' and M" respectively, the conversion factor is

$$\frac{1}{\rho}\left(1 + \frac{x\,M'}{16} + \frac{y\,M''}{16}\right).$$

Table 7 summarizes calculations of the conversion factor $\frac{1}{\rho}\left(1 + \frac{x\,M'}{16}\right)$ for a number of oxides that are formed on Ni- and Co-base superalloys.

It can be seen from Table 7 that the conversion factor is approximately the same for all the oxides considered. Use of the average value, $(0.64 \pm 0.10) \times 10^6\ m^3g^{-1}$, should produce oxide thickness estimates with limits of uncertainty of ±15%. This factor can therefore be used to estimate oxide thicknesses, to within similar limits of uncertainty, even when the identity of the oxide scale has not been resolved.

TABLE 1

CHEMICAL COMPOSITIONS (IN WEIGHT PER CENT) OF
NIMONIC 105 AND NIMONIC 75 [2]

Element / Alloy	Co	Cr	Al	Ti	Mo	Si	Cu	Fe	Mn	C	B	Zr	Ni
Nimonic 105	20 (±2)	14.5 (±1)	4.7 (±0.2)	1.2 (±0.3)	5.0 (±0.5)	1.0 max.	0.2 max.	1.0 max.	1.0 max.	0.14 (±0.02)	0.006 (±0.002)	0.10 (±0.03)	bal.
Nimonic 75	2.0 max.	19.5 (±1.5)	0.3 max	0.4 (±0.2)	0.3 max.	1.0 max.	0.5 max.	5.0 max.	1.0 max.	0.11 (±0.03)	0.001 max.	0.05 max.	bal.

TABLE 2

THE CAC BRAZING HEAT-TREATMENT CYCLE
FOR JOINING NIMONIC 105 AND NIMONIC 75 COMPONENTS [3]

Successive Holding Temperatures (K)	Intermediate Rates of Temperature Increase (K h^{-1})	Holding Time at Temperature (min)
(Ambient ($\sim$300K)		
	500	
673		15
	500	
923		10
	500	
1203		20
	500	
1313		10

TABLE 3

WEIGHT GAINS OBTAINED DURING THE OXIDATION OF NIMONIC 105 AT VARIOUS PRESSURES IN AIR, USING THE CAC BRAZING HEAT-TREATMENT CYCLE (SEE TABLE 2)

Sample(1) No.	P_{O_2} (Pa)	Area (cm^2)	Weight Gain (μg)	Specific Weight Gain (w) (μg cm^{-2})
A-1	1.4×10^{-4}	13.52	40	3.0
C-10	1.4×10^{-4}	14.48	65	4.5
C-11	2.7×10^{-4}	13.38	86	6.4
B-5	2.7×10^{-4}	13.38	220	16.4
C-12	1.4×10^{-3}	11.36	196	17.3
B-9	1.4×10^{-3}	10.26	173	17.1
B-6	2.7×10^{-3}	12.85	310	24.1
A-3	1.4×10^{-2}	13.56	530	39.1
B-7	1.4×10^{-2}	11.64	560	48.1
C-13	2.7×10^{-2}	11.60	332	28.6
B-8	5.3×10^{-2}	10.63	622	58.5
A-2	1.4×10^{-1}	13.26	890	67.1
C-14	2.7×10^{-1}	9.45	467	49.4
A-4	1.4	10.52	630	59.9
D-16	2.0×10^{4}	12.07	1845	152.9
D-17(2)	$<2.7 \times 10^{-3}$	12.29	122	9.9

(1) The letters A to D refer to the different blades (4 off) from which the samples were cut and numbered consecutively.

(2) Sample D-17 was heated in the CAC Ipsen Furnace.

TABLE 4

WEIGHT GAINS OBTAINED DURING THE OXIDATION OF NIMONIC 105 IN N_2-10% H_2 GAS AT ≈ 1.3 Pa, USING THE CAC BRAZING HEAT-TREATMENT CYCLE (SEE TABLE 2)

Sample No(1)	Area (cm^2)	Weight Gain (μg)	Specific Weight Gain (w) (μg cm^{-2})
D-18(2)	12.37	205	16.6
D-15(3)	13.20	216	16.4
D-19(3)	10.44	249	23.8

(1) See Footnote (1), Table 3.

(2) Sample D-18 was heated in the CAC Ipsen Furnace.

(3) Samples D-15 and D-19 were heated in the MRL vacuum furnace.

TABLE 5

EPMA RESULTS, APPARENT OXIDE COMPOSITIONS AND ESTIMATED TOTAL OXIDE THICKNESSES(1) FOR AIR OXIDIZED NIMONIC 105 SURFACES

Sample No.	P_{O_2} (Pa)	w (μg cm^{-2})	Calculated(1) Oxide Thickness (nm)	EPMA Beam Voltage (kV)	EPMA Results (wt.%)						Apparent Oxide Composition
					Ni	Co	Al	Ti	Cr	Mo	
A-1	1.4×10^{-4}	3.0	16	-							
C-10	1.4×10^{-4}	4.5	24	3	13	-	49	-	-	-	Al_2O_3(2)
C-11	2.7×10^{-4}	6.4	35	3	4	-	49	-	-	-	Al_2O_3(2)
B-5	2.7×10^{-4}	16.4	89	-							
C-12	1.4×10^{-3}	17.3	93	-							
B-9	1.4×10^{-3}	17.1	92	3	0.4	-	52	-	-	-	Al_2O_3(3)
B-6	2.7×10^{-3}	24.1	130	-							
A-3	1.4×10^{-2}	39.1	211	-							
B-7	1.4×10^{-2}	48.1	260	3	0.4	-	55	-	-	-	Al_2O_3(3)
C-13	2.7×10^{-2}	28.6	155	-							
B-8	5.3×10^{-2}	58.5	316	-							
A-2	1.4×10^{-1}	67.1	362	3	0.4	-	56	-	-	-	Al_2O_3(3)
C-14	2.7×10^{-1}	49.4	267	-							
A-4	1.4	59.9	324	3	0.6	0.8	57	n.d.(4)	1.1	n.d.	
				7	3.4	1.7	51	0.43	1.4	0.27	

TABLE 5

(Continued)

Sample No.	P_{O_2} (Pa)	w ($\mu g\ cm^{-2}$)	Calculated(1) Oxide Thickness (nm)	EPMA Beam Voltage (kV)	EPMA Results (wt.%)						Apparent Oxide Composition
					Ni	Co	Al	Ti	Cr	Mo	
D-16	2.0×10^4	152.9	826	15	20	7.0	18.8	1.1	2.85	2.9	Al_2O_3(5)
				20	21	9.7	10.2	1.1	2.0	3.2	
				3	13	-	26	-	-	-	
				7	10	4.6	28	4.0	0.4	0.3	Note (6)
				7	12	2	3	11	6	4	
D-17(7)	$<2.7 \times 10^{-3}$	9.9	53	3	7	4	44	n.d.	6	n.d.	Al_2O_3(2)
				7	30	16	18	1	6	3	

(1) See Appendix

(2) See Section 5.2.1. The high Ni concentrations arise from beam penetration through the thin oxide film.

(3) For Al_2O_3 the wt.% Al ≈ 53%.

(4) n.d. signifies 'not detected'

(5) See Fig. 3 and Section 5.2.1.

(6) The two 7 kV results were obtained from two visually distinct areas on the surface (see Section 6.1.1). *The first* (3 kV) and second (7 kV) analyses on D-16 were obtained from the same area.

(7) Sample D-17 was heated in the CAC Ipsen Furnace.

TABLE 6

EPMA RESULTS, APPARENT OXIDE COMPOSITIONS AND ESTIMATED TOTAL OXIDE THICKNESSES(1) FOR NIMONIC 105 SAMPLES HEATED IN N_2-10% H_2 ATMOSPHERES AT A PRESSURE OF ≈ 1.3 Pa

Sample No.	w (μg cm^{-2})	Calculated(1) Oxide Thickness (nm)	EPMA Beam Voltage (kV)	EPMA Results (wt.%)						Apparent Oxide Composition
				Ni	Co	Al	Ti	Cr	Mo	
D-18(3)	16.6	90	3	7	4	43	-	7	-	Al_2O_3(2)
			7	31	13	18	2	11	4	
D-15(4)	16.4	89	3	2	1	49	-	2	-	Al_2O_3(2)
			7	23	9	26	1	1	3	
D-19(4)	23.8	127	3	2	1	41	-	3	-	Al_2O_3(2)
			7	12	5	32	2	1	4	

(1) See Appendix

(2) See Section 5.2.1

(3) Sample D-18 was heated in the CAC Ipsen Furnace

(4) Samples D-15 and D-19 were heated in the MRL Vacuum Furnace

TABLE 7

CALCULATED VALUES OF THE CONVERSION FACTOR(1) $(1/\rho)(1 + xM'/16)$ FOR ESTIMATING THE OXIDE THICKNESS (t) FROM SPECIFIC WEIGHT GAIN (w) MEASUREMENTS

Oxide Composition	$\rho^{(2)}$ ($g\ cm^{-3}$)	M'	x	$(1/\rho)(1 + xM'/16)^{(1)}$ ($cm^3\ g^{-1}$)
Al_2O_3	3.98	27.0	2/3	0.54
Cr_2O_3	5.21	52.0	2/3	0.61
CoO	6.46	58.9	1	0.73
HfO_2	9.68	178.5	1/2	0.68
Fe_2O_3	5.20	55.9	2/3	0.64
MgO	3.58	24.3	1	0.70
NiO	6.81	58.7	1	0.69
SiO_2	2.32	28.0	1/2	0.81
Ta_2O_5	8.02	180.9	2/5	0.56
TiO_2	4.25	47.9	1/2	0.59
ZrO_2	6.10	91.2	1/2	0.63
$3\ Al_2O_3.2SiO_2$	3.2	(Al) 27.0 (Si) 28.0	6/13 2/13	0.64
$TiAl_2O_5$	3.68	(Ti) 47.9 (Al) 27.0	1/5 2/5	0.62

TABLE 7

(Continued)

Oxide Composition	$\rho^{(2)}$ (g cm^{-3})	M'	x	$(1/\rho)(1 + xM'/16)^{(1)}$ (cm^3 g^{-1})
$CoAl_2O_4$	4.37	(Co) 58.9 (Al) 27.0	1/4 1/2	0.63
Co_2SiO_4	4.68	(Co) 58.9 (Si) 28.0	1/2 1/4	0.70
$MgAl_2O_4$	3.59	(Mg) 24.3 (Al) 27.0	1/4 1/2	0.62
Mg_2SiO_4	3.22	(Mg) 24.3 (Si) 28.0	1/2 1/4	0.68
$NiAl_2O_4$	4.45	(Ni) 58.7 (Al) 27.0	1/4 1/2	0.62
Ni_2SiO_4	4.92	(Ni) 58.7 (Si) 28.0	1/2 1/4	0.67

(1) For mixed oxides, the conversion factor is $1/\rho.(1 + xM'/16 + yM''/16)$

(2) From "Engineering Properties of Selected Ceramic Materials", (ed. J.F. Lynch et al.), American Ceramic Soc. Inc., Columbus, Ohio (1966).

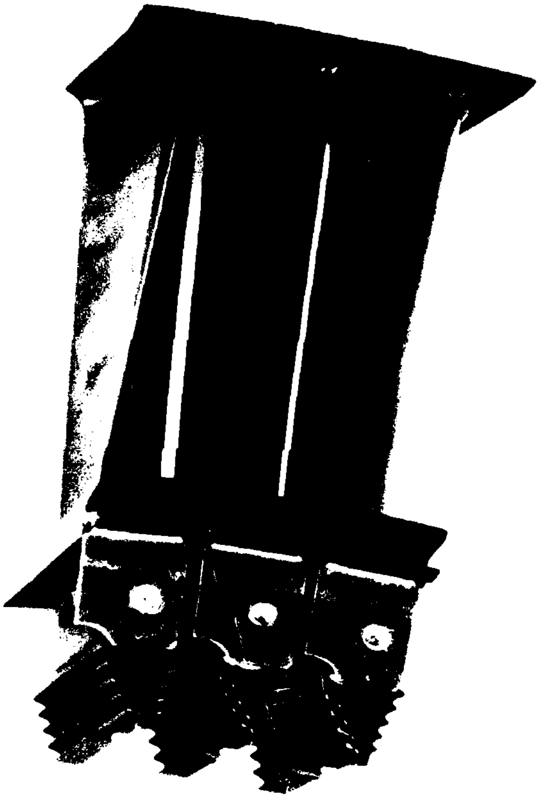

FIG. 1 - Nimonic 75 Sealing Plates Brazed on the
Leading Faces of the Fir-tree Roots of Nimonic 105 Turbine Blades

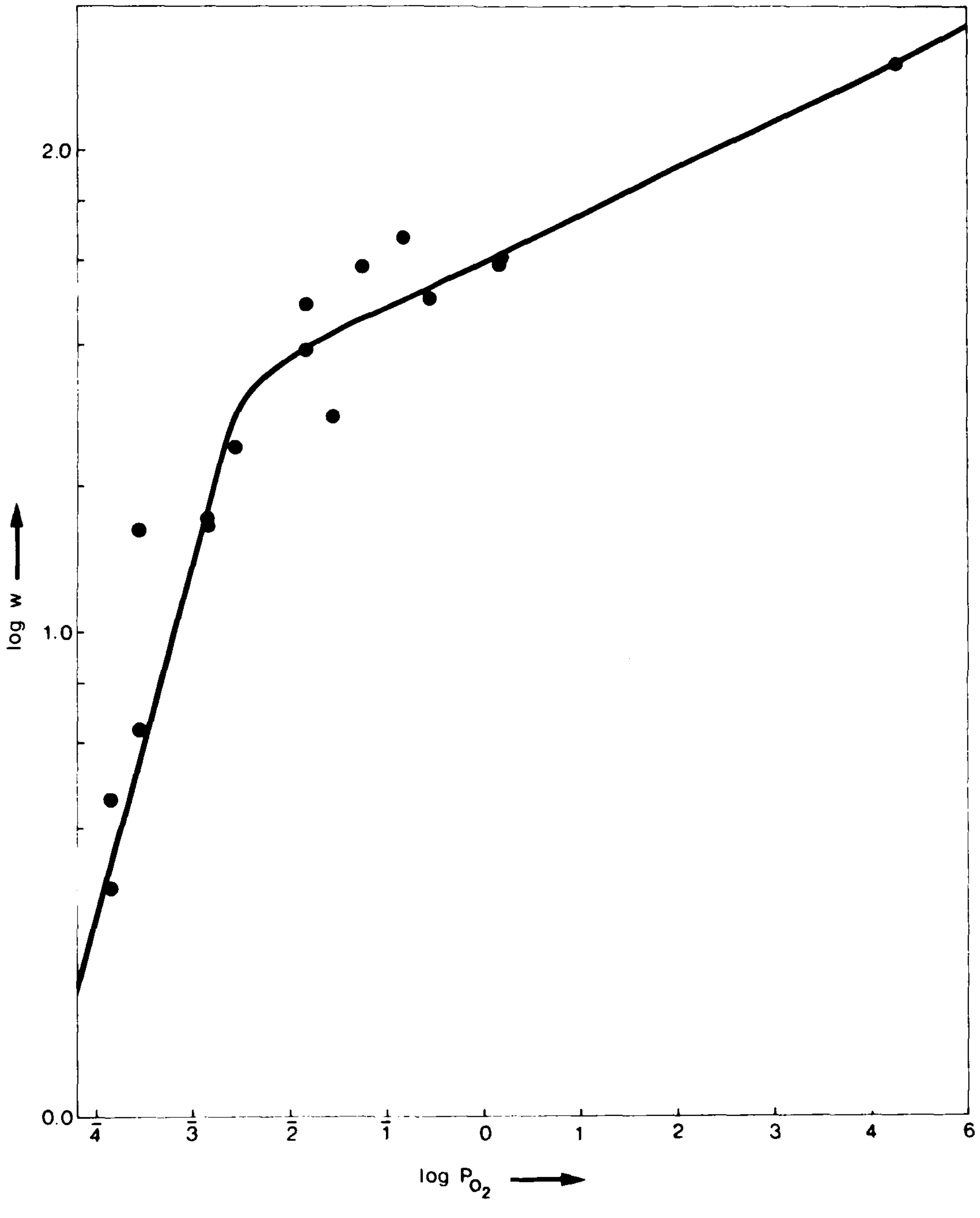

FIG. 2 - Logarithm of Specific Weight Gain w(g cm^{-2}) v. Logarithm of Oxygen Pressure P_{O_2} (Pa) for Nimonic 105

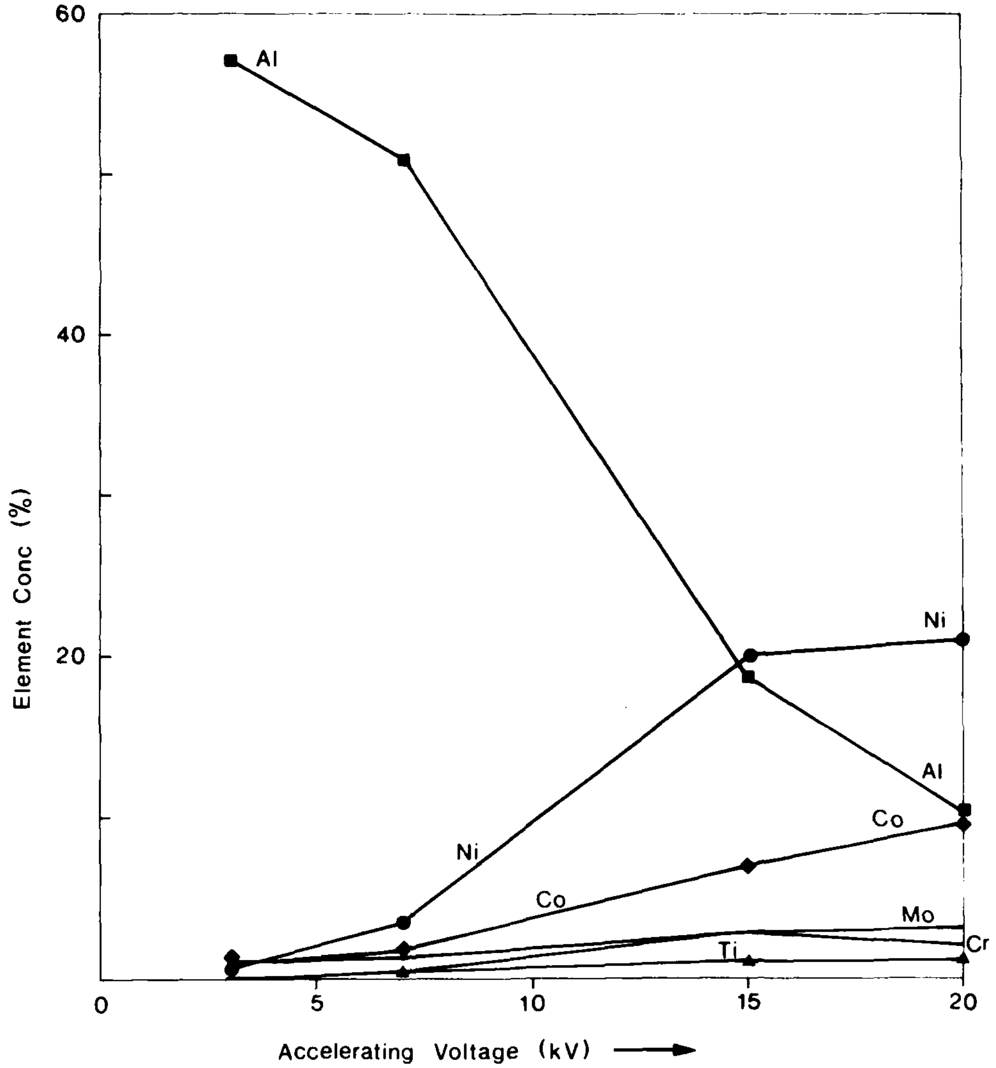

FIG. 3 - Elemental Composition (wt.%), Determined by EPMA, of the Oxidized Surface of Sample A-4 v. the Accelerating Voltage of the Incident Electron Beam (kV)

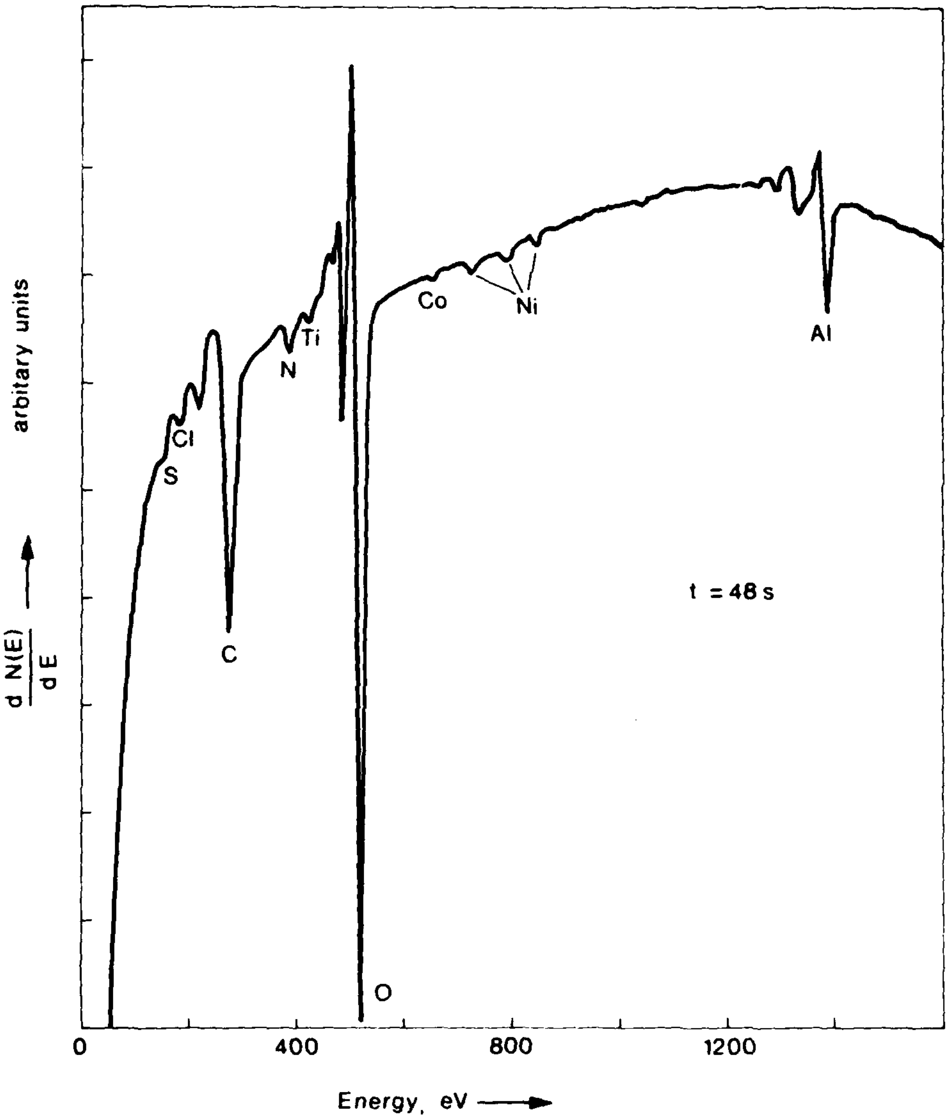

FIG. 4 - Auger Electron Spectrum for Sample C-10 After 48s of Ion Milling

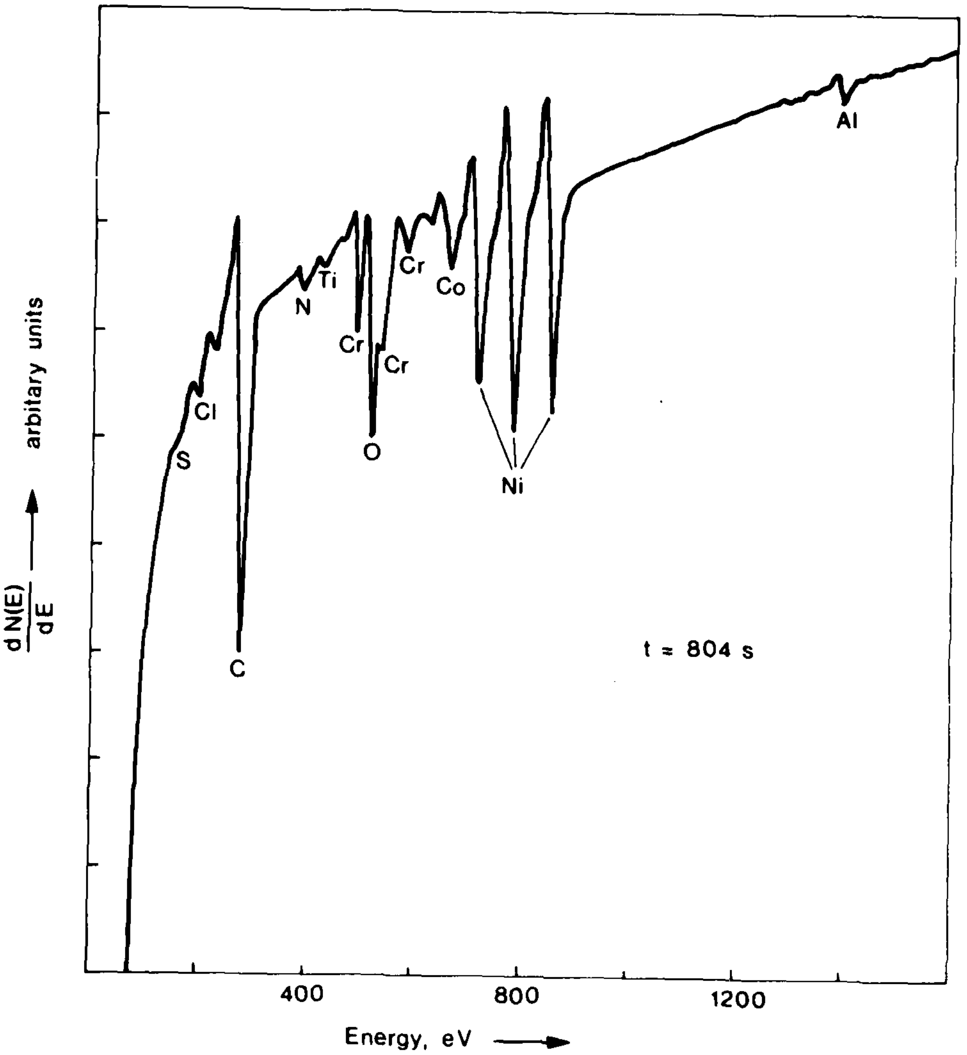

FIG. 5 - Auger Electron Spectrum for Sample C-10 After 804s of Ion Milling

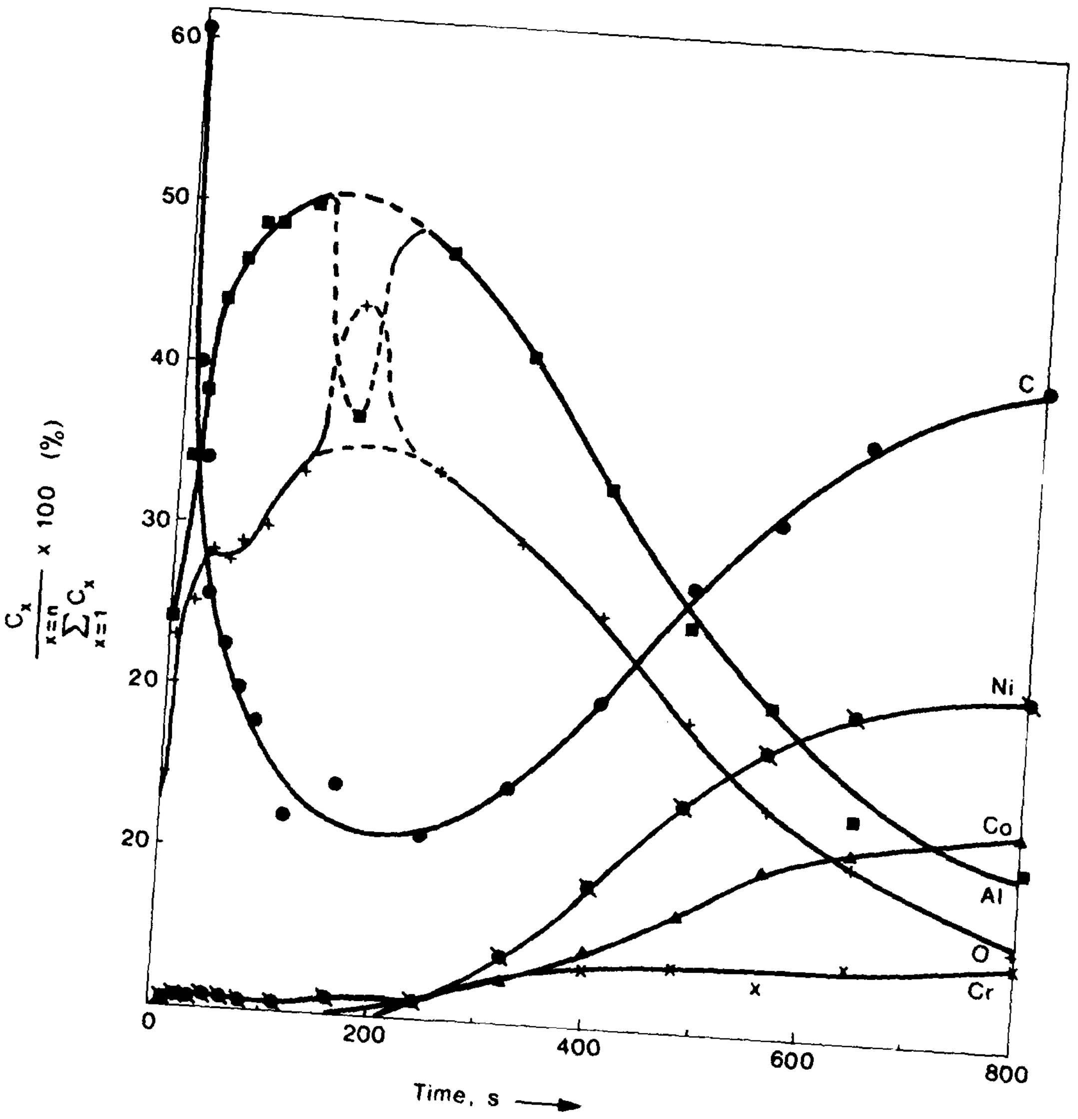

FIG. 6 - Relative Atomic Concentrations (at.%) for the Six Major Elements Detected by AES in Sample C-10 as a Function of Ion Milling Time

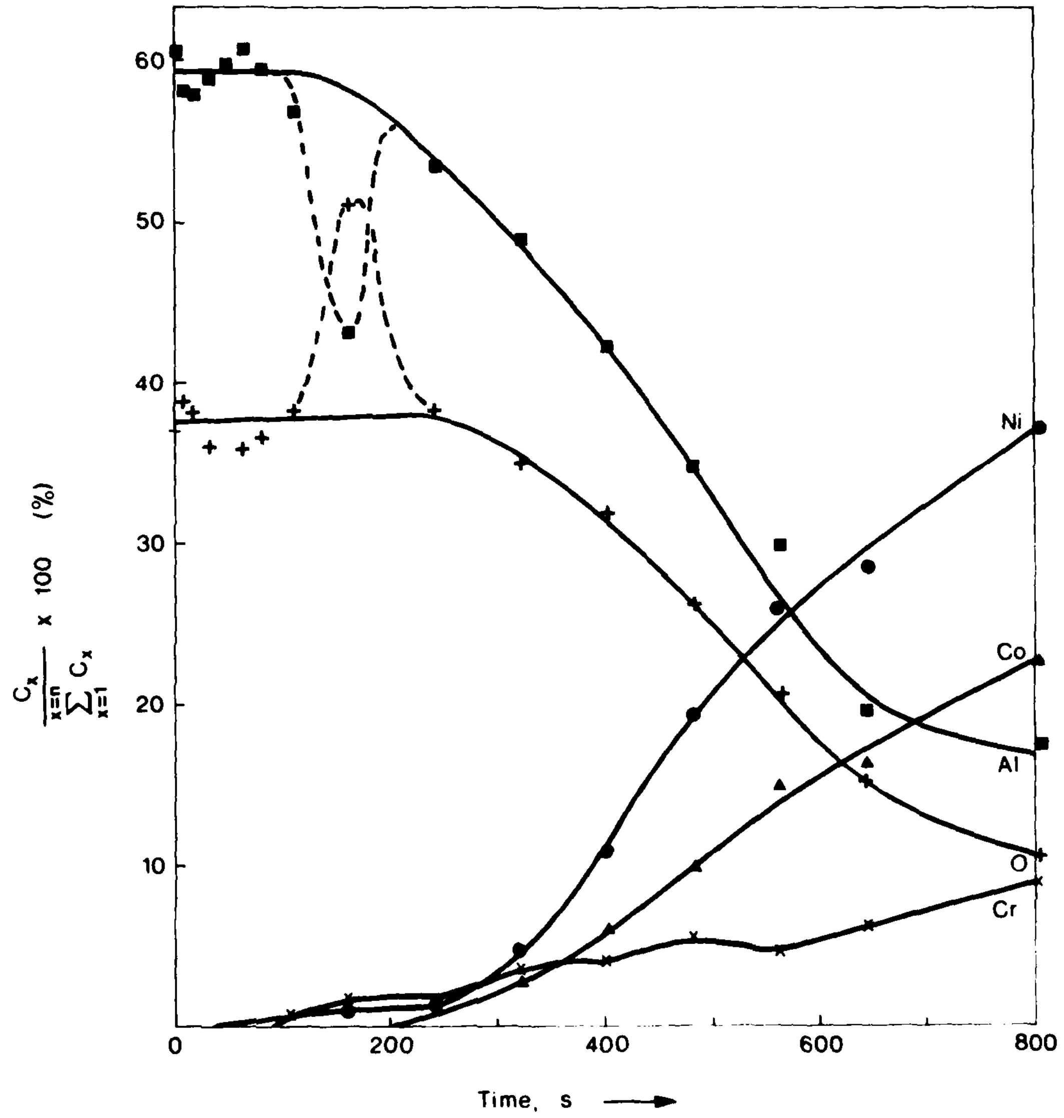

FIG. 7 - Relative Atomic Concentrations (at.%) in Sample C-10 of the Five Remaining Major Elements After Disregarding Carbon, as a Function of Ion Milling Time

DISTRIBUTION LIST

MATERIALS RESEARCH LABORATORIES

Chief Superintendent
Superintendent, Metallurgy Division
Dr. N.A. Burley
Dr. G.R. Johnston
Library
Librarian, Materials Testing Laboratories, N.S.W. Branch
 (Through Officer-in-Charge)

DEPARTMENT OF DEFENCE

Chief Defence Scientist
Deputy Chief Defence Scientist
Controller, Projects and Analytical Studies
Controller, Service Laboratories and Trials
Scientific Adviser - Army
Air Force Scientific Adviser
Naval Scientific Adviser
Chief Superintendent, Aeronautical Research Laboratories
Chief Superintendent, Weapons Systems Research Laboratory,
 Defence Research Centre
Chief Superintendent, Electronics Research Laboratory,
 Defence Research Centre
Chief Superintendent, Advanced Engineering Laboratory,
 Defence Research Centre
Superintendent, Trials Resources Laboratory, Defence Research
 Centre
Senior Librarian, Defence Research Centre
Librarian, R.A.N. Research Laboratory
Officer-in-Charge, Document Exchange Centre (16 copies)
Technical Reports Centre, Defence Central Library
Central Office, Directorate of Quality Assurance - Air Force
Deputy Director Scientific and Technical Intelligence
Head, Engineering Development Establishment
Librarian, Bridges Library, Royal Military College

DEPARTMENT OF PRODUCTIVITY

NASA Canberra Office
Head of Staff, B.D.R.S.S. (Aust.)

OTHER FEDERAL AND STATE DEPARTMENTS AND INSTRUMENTALITIES

The Chief Librarian, Central Library, C.S.I.R.O.
Australian Atomic Energy Commission Research Establishment

DISTRIBUTION LIST

(Continued)

MISCELLANEOUS - OVERSEAS

Defence Scientific and Technical Representative, Australian High Commission, London, England
Assistant Director/Armour and Materials, Military Vehicles and Engineering Establishment, Surrey, England
Reports Centre, Directorate of Materials Aviation, Kent, England
Library - Exchange Desk, National Bureau of Standards, Washington, U.S.A.
U.S. Army Standardization Representative, C/o DGAD (NSO), Canberra, A.C.T.
The Director, Defence Scientific Information & Documentation Centre, Delhi, India
Colonel B.C. Joshi, Military, Naval and Air Adviser, High Commission of India, Red Hill, A.C.T.
Director, Defence Research Centre, Kuala Lumpur, Malaysia
Exchange Section, British Library, Lending Division, Yorkshire, England
Periodicals Recording Section, Science Reference Library, The British Library, Holborn Branch, London, England
Library, Chemical Abstracts Service, Colombus, Ohio, U.S.A.
INSPEC: Acquisition Section, Institution of Electrical Engineers, Herts, England
Overseas Reports Section, Defence Research Information Centre, Orpington, Kent, England
Engineering Societies Library, New York, U.S.A.

ND